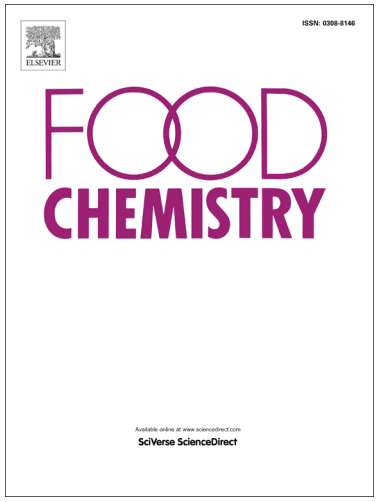

UV-C light irradiation enhances toxic effects of chlorpyrifos and its formulations

Jasmina Z. Savić, Sandra Ž. Petrović, Andreja R. Leskovac, Tamara D. Lazarević Pašti, Branislav J. Nastasijević, Brankica B. Tanović, Slavica M. Gašić, Vesna M. Vasić

PII: S0308-8146(18)31367-0
DOI: https://doi.org/10.1016/j.foodchem.2018.07.207
Reference: FOCH 23322

To appear in: *Food Chemistry*

Received Date: 11 July 2017
Revised Date: 10 April 2018
Accepted Date: 29 July 2018

Please cite this article as: Savić, J.Z., Petrović, S.Z., Leskovac, A.R., Lazarević Pašti, T.D., Nastasijević, B.J., Tanović, B.B., Gašić, S.M., Vasić, V.M., UV-C light irradiation enhances toxic effects of chlorpyrifos and its formulations, *Food Chemistry* (2018), doi: https://doi.org/10.1016/j.foodchem.2018.07.207

UV-C light irradiation enhances toxic effects of chlorpyrifos and its formulations

Jasmina Z. Savić[a,**], Sandra Ž. Petrović[a], Andreja R. Leskovac[a], Tamara D. Lazarević Pašti[a], Branislav J. Nastasijević[a], Brankica B. Tanović[b], Slavica M. Gašić[b], Vesna M. Vasić[a,*]

[a]University of Belgrade, Vinča Institute of Nuclear Sciences, Department of Physical Chemistry, P.O.B. 522, 11001 Belgrade, Serbia

[b]Institute of Pesticides and Environmental Protection, Banatska 31b, 11080 Belgrade, Serbia

Abstract

UV-C irradiation is widely used in the food industry. However, the health effects from dietary exposure to the irradiated pesticide residues retained in foodstuffs are underestimated. In this study, technical chlorpyrifos (TCPF) and its oil in water (EW) and emulsifiable concentrate (EC) formulations were irradiated by UV-C, and their photodegradation products were subjected to toxicity assessment, including determination of acetylcholinesterase (AChE) activity, genotoxicity and oxidative stress using human blood cells as a model system. Toxicity studies were performed using the chlorpyrifos concentrations in the range of those proposed as the maximum residue levels in plant commodities. TCPF, EW and EC photodegradation products induced DNA damage and oxidative stress, and their genotoxicity did not decrease as a function of irradiation time. Irradiated TCPF and EC are more potent AChE inhibitors than irradiated EW.

Accordingly, the application of UV-C irradiation must be considered when processing the plants previously treated with chlorpyrifos formulations.

Keywords

chlorpyrifos, photodegradation, acetylcholinesterase, genotoxicity, oxidative stress

Corresponding authors: *Tel: +38111 3408 287; Fax: +38111 6453 967; E-mail: evasic@vinca.rs

** Tel: +38111 3408 692; E-mail: jasnas@vinca.rs

1. Introduction

UV light technology is used widely in the food industry to prolong shelf-life, preserve nutritional value, improve the content and activity of the antioxidant compounds in fresh products and reduce the development of postharvest diseases (Turtoi, 2013). The use of non-ionizing, germicidal UV-C light is especially effective for the decontamination of the surfaces of fruits and vegetables (Turtoi, 2013). In recent years, considerable research has been devoted to the effects of UV light treatment on food safety and quality. However, one important issue that should be considered when applying UV-C irradiation is its impact on the pesticide residues retained in fruits and vegetables. Since most of the pesticides show absorption maxima at relatively short UV wavelengths (approximately 226 nm and 289 nm) (Krupa, Kickert & Jäger, 1998), the photostability of pesticides under the action of UV-C irradiation should be examined. In recent years, a growing need for pesticide use in agriculture has led to a great demand for the development and production of pesticide formulations that are safer and more convenient than previous ones (Knowles, 2008). Chlorpyrifos (CPF) (Scheme 1) belongs to a group of very effective organophosphorus pesticides (OPs) that are widely used as insecticides in agriculture, mostly for the treatment of vegetables, nut crops, and fruits as well as in forestry (MacBean, 2012). Based on the assumption that good agricultural practices are used during the application of pesticides, international organizations have established maximum residue levels (MRLs) for residues in foodstuffs (European Food Safety Authority, 2017). However, as the metabolism of CPF was not investigated for soil and seed treatments, certain tentative or existing MRLs must still be confirmed. In addition, for high oil content commodities, MRLs are also tentative due to the lack of validation data for the analytical method for enforcement (European Food Safety

Authority, 2017). The lack of the above mentioned information and an inappropriate application of CPF may lead to environmental pollution and excessive residue accumulation in the human body through the food chain, which disrupts AChE function and cause cholinergic dysfunction or even death (Colovic, 2015). Among the possible chronic effects of CPF are neurotoxicity (Hernández, González-Alzaga, López-Flores & Lacasaña, 2016), effects on reproduction (Sai et al., 2014) and cell development, particularly in the early stages of life (Muñoz-Quezada et al., 2013; Roy, Andrews, Seidler & Slotkin, 1998).

The toxic effects of CPF are attributed to irreversible inhibition of acetylcholinesterase (AChE) (Casida, 2009), as well as other enzymes important for biochemical processes (Colovic et al., 2010; Colovic, 2015; Lazarevic-Pasti, Momic, Radojevic & Vasic, 2013). Recent studies have shown that CPF induces oxidative stress through the production of free radicals and the depletion of the cellular antioxidant defense system (Ghayomi, Navaei-Nigjeh, Baeeri, Rezvanfar & Abdollahi, 2015). The enhanced production of free radicals may cause lipid peroxidation in the cell membrane, consequently disrupting its permeability and fluidity. The enhanced level of malondialdehyde (MDA), the end-product of lipid peroxidation, may lead to peroxidative damage that disturbs the structural and functional integrity of the cell membrane (Ayala, Munoz & Arguelles, 2014). The most important cellular defense mechanism against oxidative stress is mediated by antioxidative enzymes (Hundekari, Suryakar & Rathi, 2013). Catalase represents a first line of cellular antioxidative defense, and its reduced activity leads to the accumulation of H_2O_2 and consequent oxidative cellular damage. Lipid and protein oxidation as well as oxidative DNA damages may lead to inflammation and cell death (Soltaninejad & Abdollahi, 2009). Indeed, it has been reported that CPF displays teratogenic, cytotoxic and genotoxic effects

(Abdelaziz, El Makawy, Z. & Darwish, 2010; Navaei-Nigjeh et al., 2015). The genotoxic potential of CPF as observed by chromosomal loss, sister-chromatid exchanges and mitotic abnormalities has already been demonstrated in different model systems (Abdelaziz et al., 2010).

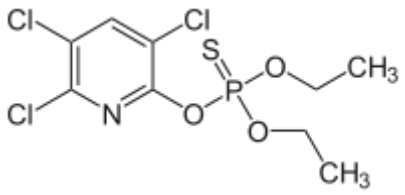

Scheme 1. The chemical structure of chlorpyrifos (CPF)

Photodegradation of pesticides does not always result in decreased activity of the parent compound. In fact, photodegradation of pesticide formulations, as mixtures of different compounds, may result in the production of more toxic products with serious health and environmental impacts than the technical material alone. Therefore, the purpose of the current study was to investigate and compare the effects of UV-C irradiation on technical CPF with the effects of UV-C irradiation on CPF formulations (emulsifiable concentrate - EC and oil-in-water emulsion - EW). The toxic effects of photodegradation products were evaluated as a function of exposure time to UV-C light by measuring the activity of AChE, genotoxicity and the parameters of oxidative stress using human peripheral blood cells as a model system. Toxicity studies of TCPF and its formulations were performed using CPF concentrations in the range of those proposed as MRLs in plant commodities.

2. Materials and Methods

2.1. Chemicals

Technical CPF (TCPF), namely, 97% CPF (minimum active substance purity) with a maximal content of the relevant impurity sulfotep of 0.3% was obtained from producer: Shenzhen Yancheng Chemicals Co. Ltd., China. The technical material of this producer is used in the production of commercially available CPF formulations RADAR 300 EC and RADAR 300 EW, both containing 300 g/L of CPF, which were obtained from Galenika Fitofarmacija AD, Belgrade, Serbia. The analytical grade standards of CPF (99.5%) and CPO (98.5%) were purchased from Dr. Ehrenstorfer GmbH (Augsburg, Germany). Acethylcholinesterase (AChE, specific activity 288 IU/mg solid, 408 IU/mg protein) from electric eel, acethylthiocholine iodide (ASChI) and 5,5'-dithio-bis-(2-nitrobenzoic acid) (DTNB) were purchased from Sigma-Aldrich (St. Louis, MO, USA). Cytochalasin B, Histopaque-1077 (Lymphocyte separation medium), thiobarbituric acid (TBA) and Giemsa stain were purchased from Merck (Darmstadt, Germany). RPMI-1640 medium, fetal bovine serum and phytohemagglutinin (PHA-M) were purchased from Fisher Scientific - UK (Leicestershire, UK). Acetonitrile, methanol and formic acid were purchased from J.T. Baker (Arnhem, Netherlands). Deionized water was used throughout.

2.2. Photodegradation studies

Photodegradation experiments were performed in an annular (double skin) photoreactor (see simplified cross section in Scheme 2). A TUV 25W mercury lamp (Philips, Eindhoven, Netherlands), which emits monochromatic UV-C radiation (λ = 254 nm), was encircled by a quartz tube (external diameter 33 mm) and two DURAN borosilicate glass tubes (41 mm (inside diameter of inner tube) and 50 mm (external diameter of outer tube)), which were sealed at both ends to enable water circulation and a constant temperature in the photoreactor during irradiation. The working solution of TCPF or one of its formulations (EW and EC) dissolved in

50% methanol was irradiated between quartz tube and inner borosilicate glass tube of the photoreactor. A 4 mL aliquot of reaction mixture, containing initially 6-9×10^{-5} M CPF in TCPF or its formulations, was taken from the photoreactor after the desired irradiation times without interrupting the UV-C irradiation. These samples were used for chromatographic analysis, as well as to compare their effects on AChE activity, genotoxicity and oxidative stress occurrence to the effects induced by the initial solutions taken from the photoreactor before irradiation began.

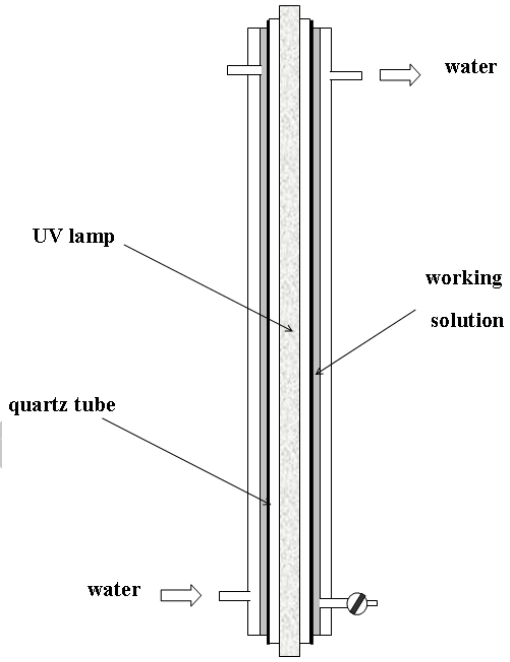

Scheme 2. Simplified crossection of photoreactor

2.3. Blood sample preparation

Blood sample were obtained from healthy, non-smoking young volunteer donors in accordance with current regulations (Parliament of the Republic of Serbia, 2005). Aliquots of heparinized

whole blood (0.5 mL) were added to culture tubes containing 4.5 mL of RPMI-1640 medium supplemented with 15% fetal bovine serum and 2% phytohemagglutinin. For the first set of experiments, the blood cultures were treated with increasing doses (0.45 µL, 4.5 µL and 45 µL) of unirradiated TCPF, EW and EC formulations, which contained initial concentrations of CPF of 7.74×10^{-5} M, 8.63×10^{-5} M and 6.95×10^{-5} M, respectively. The addition of the abovementioned doses of TCPF into cell cultures (final volume of 5 mL) lowered the CPF concentrations, which finally reached the range 6.78×10^{-9} to 6.78×10^{-7} M. The final concentrations of CPF in cell cultures treated with increasing doses of EW formulation were in the range 7.56×10^{-9} to 7.56×10^{-7} M, while upon treatment with increasing doses of EC formulation, the final concentrations of CPF in the cell cultures were in the range 6.09×10^{-9} to 6.09×10^{-7} M.

For the second set of experiments, unirradiated TCPF, EW and EC formulations at the highest dose tested were designated parent compounds. Likewise, upon irradiation, the highest doses (45 µL) of TCPF, EW and EC photodegradation products obtained at three different irradiation time points were chosen for further treatment of blood cultures. The adequate number of blood cultures per treatment was established to enable examinations of catalase activity, malondialdehyde level, micronuclei incidence and a cell proliferation index. All the investigated compounds were added to the blood cultures 24 h after they were initiated, and were present until the end of cultivation at 72 h. For the TBA and catalase assays, after 72 h of incubation, the blood cultures were separated using Histopaque-1077; the lymphocytes were collected by centrifugation, washed in physiological saline, and frozen at -80 ºC, while erythrocytes were hemolyzed in ice-cold deionized water, and frozen at -20 ºC for 24 h. The untreated cultures served as a control. The cell cultures treated with the same volume of solvent (50% methanol)

used for investigated samples (methanol final concentration in cell cultures was 0.5%), served as a positive control. No considerable differences in the estimated parameters (catalase activity, malondialdehyde level, micronuclei incidence and cell proliferation index) between the untreated control and positive control were observed. For each analysis performed, three independent experiments were carried out. Each experiment was performed using the blood sample from the different subject. The obtained data were pooled and the results are expressed as the mean and standard deviation (SD) of the mean.

2.4. Enzyme assays

2.4.1. Measurement of AChE activity

AChE activity was determined according to Ellman's procedure (Ellman, Courtney, Andres & Feather-Stone, 1961). *In vitro* experiments were performed with 2.5 IU commercially purified AChE (10 µL) from the electric eel with non-irradiated and irradiated solutions of TCPF and its formulations at 37°C in 50 mM phosphate buffer pH 8.0 (final volume 650 µL). The preincubation time of the irradiated samples in the enzyme assay was 20 min. The enzymatic reaction was initiated by the addition of acetylcholine-iodide (AChI) in combination with DTNB as a chromogenic reagent and allowed to proceed for 8 min until stopped by 10% sodium dodecyl sulfate (SDS). The product of the enzymatic reaction, thiocholine, reacts with DTNB and forms 5-thio-2-nitrobenzoate, which was spectrophotometrically determined at 412 nm. It should be noted that in these measurements, the enzyme concentration was constant and set to give an optimal spectrophotometric signal. AChE activity was determined according to the following formula:

$$\text{AChE activity} = 100 \times \frac{A_o - A}{A_o}$$

where A_o and A represent AChE activity in the absence of OP and after exposure to a given OP.

2.4.2. Measurement of catalase activity

The erythrocytes catalase activity was measured using the method of Aebi (Aebi, 1974) with minor modifications following the catalytic reduction of hydrogen peroxide. The decomposition of substrate H_2O_2 was measured spectrophotometrically at 240 nm. The activity was expressed as K - the rate constant of the first-order reaction per minute per mg of hemoglobin ($min^{-1}mg\ Hb^{-1}$). The hemoglobin concentration was determined by Drabkin's method (Cook, 1985).

2.5. Thiobarbituric acid (TBA) assay

A thawed lymphocyte suspension was treated with TBA and used to determine malondialdehyde levels spectrophotometrically at 532 nm (Aruoma, Halliwell, Laughton, Quinlan & Gutteridge, 1989). Values were expressed as nmol TBA-reactive substance (MDA equivalent)/mg protein, using a standard curve of 1,1,3,3-tetramethoxypropane. Protein concentration was determined according to the method of Lowry et al. (Lowry, Rosebrough, Farr & Randall, 1951).

2.6. Micronucleus assay

For micronuclei preparation, the cytokinesis block method of Fenech (Fenech, 2007) was used. Cytochalasin B at a final concentration 4 µg/mL was added to each culture 44 h after incubation to inhibit cytokinesis. The lymphocyte cultures were incubated for a further 28 h. Cells were collected by centrifugation and treated with hypotonic solution (0.56% KCl+0.90% NaCl, mixed

in equal volumes) at 37°C. Cell suspensions were fixed in methanol/acetic acid (3:1), washed three times with fixative and dropped onto clean slides. Slides were air-dried and stained in alkaline Giemsa. For each sample, at least 1000 binucleated cells were scored, and micronuclei were recorded using a microscope.

2.7. Cell proliferation index

A cytokinesis-block proliferation index (CBPI) was calculated as follows: CBPI = $[M_I + 2M_{II} + 3(M_{III} + M_{IV})]/N$, where M_I-M_{IV} represents the number of cells with one to four nuclei, and N is the number of cells scored (Surralles, Xamena, Creus, Catalan, Norppa & Marcos, 1995).

2.8. Statistics

Statistical analysis was performed using the Student's *t* test and product-moment and partial correlations with the software package Statistica 8 and OriginPro 8.5.1 for Microsoft Windows. *P* values less than 0.05 were considered significant.

2.9. Apparatus

The spectrophotometric measurements related to enzymatic assays and oxidative stress investigation were performed using a PE Lambda 35 spectrophotometer. A Waters ACQUITY Ultra Performance Liquid Chromatography (UPLC) system with a PDA detector and a BEH C_{18}, 1.7 µm, 100 mm×2.1 mm column (Waters) as a stationary phase was used for chromatographic separation of reaction mixtures during the photodegradation process. All analyses were performed using a gradient condition (see Table 1S) with a mobile phase consisting of solvent A (0.1 wt. % HCOOH in water) and solvent B (0.1 wt. % HCOOH in acetonitrile) at a constant

flow rate of 0.3 mL/min. The autosampler and column compartment were maintained at 4°C and 30°C, respectively. The 3D data (absorbance vs. time and wavelength) were recorded in from 210 to 400 nm and 2D chromatograms at 280 nm. The run time was 8 min, and the injection volume was 3.5 µL. A Waters UPLC system with Tandem Quadrupole Detector (LC/MS) was used to identify the main hydrolysis product, 3,5,6-trichloro-2-pyridinol (TCP). The conditions for obtaining mass spectra for LC/MS in ESI negative mode were: source temperature 150°C, desolvation temperature 350°C, capillary voltage 4 kV, cone voltage 25 V, desolvation gas flow 700 L/h, m/z in the range from 50 to 500. The same chromatographic gradient profile was used as in the UPLC/PDA experiments. Data were obtained and processed using MassLynx 4.1 software. The micronuclei were recorded using an Optech microscope (Munich, Germany) with 400× or 1000× magnification.

3. Results and Discussion

3.1. Photodegradation of CPF in TCPF, EC and EW formulations

Three forms of CPF (TCPF and its two formulations), containing approximately 10^{-5} M CPF were exposed to the UV-C lamp in the photoreactor at ambient temperature. Because of the low CPF solubility in water, 1:1 methanol/water solutions (pH ~ 6.5) (Castells, Rafols, Roses & Bosch, 2003) were used in all experiments. The course of photodegradation was followed chromatographically as a function of irradiation time. As an example, the UPLC chromatograms of the TCPF solution containing an initial concentration of 7.74×10^{-5} M CPF, recorded after 0, 14, 36, 80 and 180 min exposure to UV-C light in photoreactor, are shown in Fig. 1. Like other

OPs, CPF is characterized by a thione moiety (P=S) and three –OR groups (Casida, 2009). This pesticide undergoes chemical transformation after metabolic oxidation, which leads to oxon derivative formation, where sulfur from the thionate group is replaced by an oxygen (Kulkarni & Hodgson, 1980). Both CPF and its oxo-analogue CPO were identified in the chromatogram of their analytical standards (Fig. 1, inset), with the chromatographic peaks at 4.2 min, and 3.4 min, respectively. The time-dependent disappearance of CPF and appearance/disappearance of CPO obtained due to irradiation process were observed. In the supplementary file, the absorption spectrum of CPF is presented in Fig. 1S.

Fig. 1.

According to the UPLC chromatograms of TCPF (Fig. 1a-e) and the investigated formulations (Fig. 2Sa, b), it was obvious that the content of reaction mixture was depended on irradiation time and varied during the course of photodegradation. In Table 2S, the hourly decrease in CPF in the TCPF, EC and EW formulations according to irradiation progress is presented. The solutions of TCPF, EC and EW formulations containing the same concentration of CPF as the corresponding irradiated samples, but without exposure to UV-C light (control samples in the dark), were also followed chromatographically for 4 h. During this time, the decrease in CPF concentration was less than 4.5%. According to these findings, it was obvious that all changes in the content of reaction mixtures can be ascribed to the action of UV-C light. Our results confirmed that the transformation of CPF to CPO was due to irradiation of the investigated samples in the photoreactor by UV-C light, as also found in a previous study (Bavcon Kralj,

Franko & Trebse, 2007) which showed that in a 60 min experiment, the maximally observed amount of CPO did not exceed 1% of the parent compound.

The concentrations of CPF and CPO in the present experiment were determined from 2D chromatographic data recorded at 280 nm using calibration graphs constructed by applying the series of solutions with known concentrations of CPF and CPO pure standards (Fig. 3S) and are presented in Table 3S. The maximal CPO concentrations for TCPF and EC, achieved approximately after 80 min of UV-C irradiation, were higher than 1% (1.65% and 1.38%, respectively) of the initial CPF concentration in the solution before irradiation. For the EW formulation, the maximal observed CPO concentration (0.73% of initial CPF concentration) was achieved after 17 min of UV light exposure. Spontaneous CPF hydrolysis also occurred during irradiation. Moreover, the main hydrolysis product of CPF, TCP was detected by LC/MS (Fig. 4S), as also found in other studies (Bavcon Kralj et al., 2007; Zabar, Sarakha, Lebedev, Polyakova & Trebse, 2016). According to the literature data (Bavcon Kralj et al., 2007; Zabar et al., 2016), TCP was formed during irradiation and was transformed to other products due to its low photostability.

The decrease in CPF concentration with time fits a single exponential function very well in all cases (Fig. 5S). The pseudo-first order rate constants (k_{obs}) for CPF disappearance, determined from pseudo-first order kinetic curves representing dependence of CPF concentration on irradiation times, are 1.97×10^{-4} s^{-1} (TCPF), 3.81×10^{-4} s^{-1} (EW) and 1.63×10^{-4} s^{-1} (EC). The rate of CPF photodegradation was similar in the TCPF and EC formulations but approximately twice as high in the EW formulation. This finding is in accordance with the time-dependent change in

CPO concentration. CPO concentration reached its maximum after approximately 25 min irradiation for the EW formulation, and after approximately 75 – 100 min for TCPF and EC formulations (Fig. 5S). Both the EC and EW formulations are fairly complex materials, that contain various ingredients (surfactants, solvents, emulsifiers, anti-freeze…), which apparently interfered with CPF during UV irradiation. The CPF/CPO concentration ratio and kinetic results are the consequence of formulation composition, since each organic molecule of inert ingredients could be degraded, likely in competition with the active substance and may act as a possible photosensitizer or quencher. However, in this investigation, we used toxicity studies to investigate and compare the toxicity of the technical material CPF and its formulations before and after their exposure to UV-C irradiation.

3.2. Effect of irradiation on AChE activity

To estimate the potency of TCPF, EW and EC formulations to inhibit AChE before irradiation, the *in vitro* activity of the target enzyme was investigated using a series of solutions containing CPF concentration ranging from 10^{-8} to 10^{-5} M. The inhibition curves of TCPF, EW and EC, together with the inhibition curves of the analytical standards of CPF and CPO are presented in Fig. 2a.

Fig. 2.

Analytical grade CPF (Fig. 2, curve 4) is a slightly more potent inhibitor of AChE in the investigated concentration range, compared to TCPF and EC containing the same initial CPF

concentration. EW formulation induced more intensive AChE inhibition, even at low CPF concentrations in this formulation. For example, 4.2×10^{-6} M CPF in the EW formulation induced 61.6% of AChE inhibition, while for the TCPF, EC formulation and CPF standard, the corresponding AChE inhibitions for the same CPF concentration were 32.9%, 23.6% and 47.0%, respectively.

The difference in the inhibitory efficiency of the studied formulations before irradiation can be attributed to their different initial compositions. Both formulations contain sulfotep, TCP and phosphothioates (Ahmed, Ahmed, Saleh & Ismail, 2010; Suvarchala & Philip, 2016). According to FAO Specifications and Evaluations for CPF, the content of these impurities is below 1, i.e., 0.3% of CPF content. Although toxic (IC_{50} for AChE inhibition is 1×10^{-5} M) (Wood & Osborne, 1991), the sulfotep contribution to AChE inhibition is negligible due to its low concentration in the measured samples. EW formulation consists of an active substance dissolved in water-immiscible solvent, which is dispersed as fine oil-phase droplets in water in the presence of surfactants (Gašić, Brkić, Radivojević & Tomašević, 2012). These surfactants, in combination with neurotoxic petroleum hydrocarbons and 1-methoxy-2-propanol (glycolether) could induce additional AChE inhibition (ECETOC, 2005; Holth & Tollefsen, 2012). The inhibition curve of CPO, the oxidation product of CPF found in all formulations due to irradiation, suggests that it is more toxic than the parent compound (Casida, 2009). The results presented in Table 3S indicate that the highest CPO concentrations achieved due to irradiation were 1.20×10^{-6}M, 6.34×10^{-7} M and 9.62×10^{-7} M for TCPF, EW and EC, respectively. Based on the CPO inhibition curve (Fig. 2a, curve 5), it can be concluded that CPO formed in studied preparations can inhibit up to 95%, since the remaining CPF could inhibit up to 40% of the initial AChE activity.

The influence of photodegraded samples on AChE activity as a function of irradiation time is shown in Fig. 2(b-d). The initial AChE activity decreased and the highest inhibition for TCPF and EC (20% and 10% reminded initial activity, respectively) was accomplished after 50-60 min irradiation. With prolonged irradiation time, AChE activity increased to approximately 40% of its initial value. Taking into account these findings, it can be concluded that the reduced activity of the enzyme due to the irradiation is mostly due to CPF and the formation of CPO. This is also in accordance with results obtained using a 125 W xenon parabolic lamp for CPF degradation (Bavcon Kralj et al., 2007). However, the initial AChE activity is approximately 20% lower in the presence of the EW formulation before irradiation when considering the present CPF concentration. This value increased continually with irradiation time.

To better understand the observed differences, the results presented in Figs. 2b, 2c and 2d were analyzed. It is obvious that CPF concentration decreased in all cases up to approximately 0.25×10^{-5} - 1×10^{-5} M. This remaining CPF concentration can induce up to 20% of enzyme inhibition in the AChE assay (Fig. 2a). However, CPO concentration increased with the time of irradiation and then decreased. It achieved a maximal level with a plateau within 70 - 80 min for TCPF, 20 - 40 min for EW and 60 - 120 min for EC. This increase in CPO concentration is in accordance with the highest percent enzyme inhibition achieved after mentioned irradiation times, which produced the highest level of CPO concentration for the selected formulation. While the TCPF and EC formulations behave similarly, significant differences are observed for EW formulation. In this formulation, the rate of CPO formation is highest, but its maximal concentration is lowest. It also corresponded to the lowest decrease in initial AChE activity

within the whole irradiation period. However, although CPO almost completely disappears after 150 min, approximately 30% of the initial enzyme activity was lost. The decrease in the initial AChE activity in all formulations after 200 min irradiation can be ascribed to the remaining CPF concentration in the medium (below 2.6×10^{-6} M), as well as the formation of different CPF and CPO isomers with unknown inhibition capacities (Bavcon Kralj et al., 2007). Moreover, our previous study showed the antagonistic effect of mixtures containing CPF and CPO on AChE inhibition (Colovic, Krstic, Uscumlic & Vasic, 2011).

However, the ingredients of the EC formulation do not influence the CPF degradation rate or AChE activity (Knowles, 2008). Rather, our results indicate that the constituents of EW formulation affect both the rate of degradation and AChE activity. As stated above (Table 3S), the EW formulation showed the lowest percentage of CPF transformed to CPO, which in practice means that for this formulation, photochemical treatment could be the best choice for wide usage in terms of potential toxic effects, as well as for those who remove the EW formulation in this way.

3.3. Effects of irradiated TCPF, and EW and EC formulations on parameters of oxidative stress

3.3.1. Effect of irradiation on MDA level

In the first set of experiments for MDA level evaluation, the cell cultures were treated with increasing doses (0.45 µL, 4.5 µL and 45 µL) of unirradiated TCPF, EW and EC formulations for 72 h (Fig. 3a). The results have shown that unirradiated TCPF, EC and EW formulations

caused a concentration-dependent increase in MDA level compared to the untreated control ($p < 0.05$). The maximal enhancement of the MDA level was achieved at the highest dose of TCPF applied. Both the EW and EC formulations induced significantly lower levels of MDA compared to the pure active substance ($p < 0.05$). However, the results also show that EC formulation is a more potent inducer of oxidative stress than EW formulation. Thus, it can be concluded that CPF is responsible for increased MDA level, while the ingredients of the EW and EC formulations have partially attenuated the CPF toxic effects.

Fig. 3.

Since considerable differences between the TCPF, EC, and EW formulations were observed at the highest dose applied (45 µL), this dose was chosen for further experiments. Therefore, in the second set of experiments, cell cultures were treated with the highest dose of irradiated TCPF, EW and EC formulations, and their effects were compared to the effects induced by corresponding parent compounds (unirradiated TCPF, EC and EW formulations at the highest dose applied; see section 2.3.). The dependence of the MDA level and the CPF and CPO concentrations on irradiation time are presented in Fig. 3 (b-d).

In lymphocytes treated with irradiated TCPF, EC and EW formulations, a time-dependent alteration of MDA level compared to unirradiated parent compounds was observed. Similar behavior in the TCPF and EC formulation was observed. Namely, within the first 13-17 min of irradiation, the MDA level significantly decreased compared to the parent compound, while at subsequent time points an increase of MDA level was observed ($p < 0.05$). The maximum MDA

level overlapped with the maximum CPO concentration formed due to irradiation. It was shown that CPO formation rate is lower in TCPF and EC formulations (Section 3.1). The conclusion can be made that the decrease in MDA level at the first time point was due to the decrease of CPF concentration during irradiation. It appears that CPO's influence on MDA level is significantly stronger, and its formation in the TCPF and EC formulations induced a further increase in MDA level. The irradiated EW samples induced a significant increase in MDA level ($p < 0.05$) even at the first time point of irradiation, which then decreased as a function of irradiation time. This behavior is in accordance with the time-dependent formation of the CPO, the maximal concentration of which was achieved at the same time point when the maximal MDA level was observed. Notably, the MDA level reached ~ (100±10) % after approximately 200 min in all cases, i.e., after almost complete CPF and CPO degradation. These findings suggest that other constituents of the studied formulations did not significantly affect the oxidative processes on the cell membrane.

3.3.2. Effect of irradiation on catalase activity

The activity of erythrocyte catalase was measured in blood cultures cultivated in the presence of unirradiated and irradiated TCPF, EW and EC formulations using the same experimental set-up used for the measurement of MDA level. As shown in Fig. 4a, the unirradiated TCPF and EC formulation behaved in a similar manner. However, in all treatments performed with increasing doses of TCPF, EW and EC formulations, the activity of catalase was similar to that of the untreated control.

Fig. 4.

After irradiation, it was observed that the photodegradation products of the TCPF, EW and EC formulations did not have a significant influence on catalase activity compared to the parent compounds (Fig. 4 (b-d)).

3.4. Genotoxicity (incidence of micronuclei and cell proliferation index) induced by irradiated TCPF, and EW and EC formulations

The genotoxic effects of unirradiated and irradiated TCPF, EW and EC formulations in human lymphocytes were evaluated using the CBMN test, which is a reliable and accurate method for measuring chromosome damage, including both chromosome loss and chromosome breakage, that can provide accurate information on cell cycle progression and cytotoxicity (Fenech, 2007). Using the same experimental set-up using for the previous analysis, the results obtained in the first set of experiments showed that unirradiated TCPF, EW and EC formulations displayed genotoxic effects, as revealed by significant enhancement of the micronuclei incidence and a decline in cell proliferation in a concentration-dependent manner ($p < 0.05$) (Fig. 5a and 6a). Correlation analysis has shown that the incidence of micronuclei and cell proliferation potential were correlated inversely ($p < 0.005$).

Fig. 5.

Fig.6.

TCPF behaved as a more powerful genotoxic inducer than EW and EC formulations, generating high micronuclei incidence and proliferation suppression even at low concentrations. This effect can be ascribed to CPF and impurities present in the technical material. Since TCP is reported to be less toxic than CPF, we assumed that sulfotep contributed to the observed toxicity. Sulfotep (max 0.3%) is the relevant impurity in technical material of CPF (min active substance concentration is 97%) (FAO, 2008; WHO, 2015). According to toxicity studies conducted for CPF technical material evaluation, the acute oral LD_{50} of sulfotep is 5 mg/kg of body weight (bw), while for CPF it is 229 mg/kg bw (FAO, 2008). Furthermore, the obtained results clearly showed a positive correlation between the level of MDA and the incidence of micronuclei ($p < 0.05$) indicating the oxidative damage to DNA. The EW and EC formulations also induced significantly higher micronuclei incidence compared to the untreated control, but to a lesser extent than for TCPF. Possibly, the different additives presented in formulations can reduce their genotoxic potential compared to the technical material.

Results obtained from the second set of experiments have shown that irradiation of TCPF has yielded products with similar or even greater genotoxic potency than the parent compound (Figs. 5 (b-d) and 6 (b-d)). The exception is a product generated at the second time point of irradiation, which decreased micronuclei incidence and enhancement of cell proliferation compared to the parent compound. It appears that the maximal concentration of CPO formed during irradiation was more prone to induce lipid peroxidation than DNA damage. Despite its oxidizing potential, this product was a weaker inducer of DNA damage than the parent compound but is still genotoxic compared to the untreated control.

During the photodegradation of the EW formulation (Figs. 5 (b-d) and 6 (b-d)), the products formed at the first and at second time point of irradiation caused a significant reduction in micronuclei incidence and increase in cell proliferation potential ($p < 0.05$) compared to the parent compound. These effects can be ascribed to the time-dependent formation of the CPO, similar to effects observed in the treatments with irradiated TCPF. However, the product formed at the end of the irradiation process displayed similar genotoxic potency to the parent compound due to residual CPF and possibly other constituents of this formulation. Considering the photodegradation of the EC formulation, similarly, all products formed during irradiation attenuated the micronuclei incidence ($p < 0.05$) while maintaining an almost unchanged cell proliferation potential compared to the parent compound (Figs. 5 (b-d) and 6 (b-d)).

Statistical analysis of the results showed that all the products of EW and EC irradiation were genotoxic compared to the untreated control, inducing either an increase in micronuclei incidence or suppression of cell proliferation ($p < 0.05$).

Taken together, the results presented above suggest that CPF is characterized by high potency to induce lipid peroxidation, enhancement of micronuclei and suppression of cell proliferation, whereas CPO is more prone to induce lipid peroxidation, with no high potential to induce DNA damage.

In general, the photodegradation products of TCPF, EW and EC formulations obtained at all investigated irradiation time points induced oxidative stress and/or DNA damage, and thus their

genotoxicity did not decrease as a function of irradiation time. Similar findings were obtained in our previous investigation of diazinon and its photodegradation products (Colovic et al., 2010). It is worth noting that the discrepancy between the effects induced by TCPF and both of formulations can be attributed to their constituents, which moderate the cellular response to TCPF.

4. Conclusion

The photodegradation of chlorpyrifos from TCPF and two commercially available formulations (EC and EW) induced by UV-C light was investigated to compare the toxicity of these three forms of CPF before and after exposure to UV-C irradiation. In all cases, CPF almost completely disappeared within three hours. However, the irradiation of all samples was followed by the time-dependent change in their toxicity. CPF concentration decreased during UV-C irradiation, but the concentration of CPO, identified as the transformation product of CPF, increased, reaching a maximal concentration after approximately 17 min (EW) and 80 min (TCPF and EC) of irradiation, and then decreased.

The significant AChE inhibition induced by the irradiated TCPF and EC formulations was noticed at irradiation times up to 100 min, with maximal inhibition induced by samples taken from the reactor after 40-50 min of UV-C irradiation. These changes were ascribed to CPO formation, followed by its further degradation during photodegradation, which led to increased AChE inhibition. However, irradiation decreased AChE activity inhibition induced by EW formulation due to a higher rate of CPF and CPO degradation. A subsequent increase of AChE activity in the presence of irradiated samples was likely due to the hydrolysis of CPF and CPO-

forming TCP, which is not an inhibitor of AChE activity. The EW formulation showed that the lowest percentage of CPF transformed to CPO (Table 3S), which indicates that this formulation is the best choice for wide usage due to the constant decrease in toxicity during photochemical treatment.

In terms of the potency to induce oxidative stress, the unirradiated TCPF, EC and EW formulations significantly enhanced the MDA level in a concentration-dependent manner compared to the untreated control. At higher applied concentrations, the TCPF and EC behaved in a similar manner and were more potent inducers of oxidative stress than the EW formulation. In the genotoxicity assessment, it was observed that the TCPF, EC and EW formulations induced DNA damage, as revealed by a significant enhancement of the micronuclei incidence and a decline in cell proliferation compared to the untreated control. The photodegradation of TCPF, EC and EW formulations, independent of irradiation length, yielded the products that induced the oxidative stress and/or DNA damage, which demonstrates that their genotoxicity did not decrease as a function of irradiation time. Notably, the TCPF behaved as a more powerful genotoxic inducer than the EW and EC formulations. Taken together, the results of the current study demonstrate that caution should be used when applying UV-C irradiation in the food industry for the treatment of fruits and vegetables previously treated with CPF formulations.

Acknowledgement

This work was supported by the Ministry of Education, Science and Technological Development of the Republic of Serbia (Grant no. 172023).

CONFLICT OF INTEREST

The authors confirm that this article content has no conflict of interest.

References

Abdelaziz, K. B., El Makawy, A. I., Z., E. A., & Darwish, A. M. (2010). Genotoxicity of chlorpyrifos and the antimutagenic role of lettuce leaves in male mice. *Comunicata Scientiae 1*(2), 137-145.

Aebi, H. (1974). Catalase. In: H. U. Bergmeyer, *Methods of Enzymatic Analysis*. Weinheim: Verlag Chemie.

Ahmed, M. H. M., Ahmed, I. S., Saleh, M. A., & Ismail, I. I. (2010). The Quality of Chlorpyrifos Emulsifiable Concentrate Formulations. *Journal of Applied Sciences Research, 6*(8), 1202-1207.

Aruoma, O. I., Halliwell, B., Laughton, M. J., Quinlan, G. J., & Gutteridge, J. M. (1989). The mechanism of initiation of lipid peroxidation. Evidence against a requirement for an iron(II)-iron(III) complex. *Biochemical Journal, 258*(2), 617-620.

Ayala, A., Munoz, M. F., & Arguelles, S. (2014). Lipid peroxidation: production, metabolism, and signaling mechanisms of malondialdehyde and 4-hydroxy-2-nonenal. *Oxidative Medicine and Cellular Longevity, 2014*, 360438.

Bavcon Kralj, M., Franko, M., & Trebse, P. (2007). Photodegradation of organophosphorus insecticides – Investigations of products and their toxicity using gas chromatography–mass spectrometry and AChE-thermal lens spectrometric bioassay. *Chemosphere, 67*, 99-107.

Casida, J. E. (2009). Pest toxicology: the primary mechanisms of pesticide action. *Chem Res Toxicol, 22*(4), 609-619.

Castells, C. B., Rafols, C., Roses, M., & Bosch, E. (2003). Effect of temperature on pH measurements and acid-base equilibria in methanol-water mixtures. *Journal of Chromatography A, 1002*, 41-53.

Colovic, M., Krstic, D., Petrovic, S., Leskovac, A., Joksic, G., Savic, J., Franko, M., Trebse, P., & Vasic, V. (2010). Toxic effects of diazinon and its photodegradation products. *Toxicol Lett, 193*(1), 9-18.

Colovic, M. B., Krstic, D. Z., Uscumlic, G. S., & Vasic, V. M. (2011). Single and simultaneous exposure of acetylcholinesterase to diazinon, chlorpyrifos and their photodegradation products. *Pesticide Biochemistry and Physiology, 100*(1), 16-22.

Colovic, M. B., Lazarevic-Pašti, T.D., Vasic, V.M. (2015). Toxic effects of chlorpyrifos and its metabolites on some physiologically important enzymes: Atpases, cholinesterases, peroxidases. *Chlorpyrifos: Toxicological Properties, Uses and Effects on Human Health and the Environment* (pp. 87-140): Nova Science Publishers, Inc.

Cook, J. D. (1985). *Measurements of iron status: a report of the International Nutritional Anemia Consultative Group (INACG)*. Washington, DC, USA: Nutrition Foundation.

ECETOC (2005). The toxicology of glycol ethers and its relevance to man, Fourth edition, Volume I. *ECETOC Technical Report* (pp. 1-207). Brussels.

Ellman, G. L., Courtney, K. D., Andres, V., Jr., & Feather-Stone, R. M. (1961). A new and rapid colorimetric determination of acetylcholinesterase activity. *Biochem Pharmacol, 7*, 88-95.

European Food Safety Authority, A. B., D. Brocca, C. De Lentdecker, Z Erdos, L. Ferreira, L. Greco, S. Jarrah, D. Kardassi, R. Leuschner, C. Lythgo, P. Medina, I. Miron, T. Molnar, A. Nougadere, R. Pedersen, H. Reich, A. Sacchi, M. Santos, A. Stanek, J. Sturma, J. Tarazona, A. Theobald, B. Vagenende, A. Verani and L. Villamar-Bouza (2017). Reasoned opinion on the review of the existing maximum residue levels for chlorpyrifos according to Article 12 of Regulation (EC) No 396/2005. *EFSA Journal, 15*(3), 4733-4853.

FAO (2008). FAO SPECIFICATIONS AND EVALUATIONS FOR AGRICULTURAL PESTICIDES: CHLORPYRIFOS (pp. 1-46).

Fenech, M. (2007). Cytokinesis-block micronucleus cytome assay. *Nature Protocols*, *2*(5), 1084-1104.

Gašić, S., Brkić, D., Radivojević, L., & Tomašević, A. (2012). Development of water based pesticide system. *Pestic. Phytomed. , 27*(1), 77-81.

Ghayomi, F., Navaei-Nigjeh, M., Baeeri, M., Rezvanfar, M. A., & Abdollahi, M. (2015). A mechanistic approach for modulation of chlorpyrifos-induced toxicity in human lymphocytes by melatonin, coenzyme Q10, and vinpocetine. *Human and Experimental Toxicology*, *35*, 839-850.

Hernández, A. F., González-Alzaga, B., López-Flores, I., & Lacasaña, M. (2016). Systematic reviews on neurodevelopmental and neurodegenerative disorders linked to pesticide exposure: Methodological features and impact on risk assessment. *Environment International*, *92-93*, 657-679.

Holth, T. F., & Tollefsen, K. E. (2012). Acetylcholine esterase inhibitors in effluents from oil production platforms in the North Sea. *Aquatic Toxicology*, *112-113*, 92-98.

Hundekari, I. A., Suryakar, A. N., & Rathi, D. B. (2013). Acute organo-phosphorus pesticide poisoning in North Karnataka, India: oxidative damage, haemoglobin level and total leukocyte. *African Health Sciences*, *13*(1), 129-136.

Knowles, A. (2008). Recent developments of safer formulations of agrochemicals *Environmentalist*, *28*(1), 35-44.

Krupa, S. V., Kickert, R. N., & Jäger, H. J. (1998). *Elevated Ultraviolet (UV)-B Radiation and Agriculture*. Berlin Springer.

Kulkarni, A. P., & Hodgson, E. (1980). Metabolism of insecticides by mixed function oxidase systems. *Pharmacol Ther*, *8*(2), 379-475.

Lazarevic-Pasti, T., Momic, T., Radojevic, M. M., & Vasic, V. (2013). Influence of organophosphorus pesticides on peroxidase and chlorination activity of human myeloperoxidase. *Pesticide Biochemistry and Physiology*, *107*(1), 55-60.

Lowry, O. H., Rosebrough, N. J., Farr, A. L., & Randall, R. J. (1951). Protein measurement with the Folin phenol reagent. *Journal of Biological Chemistry*, *193*(1), 265-275.

MacBean, C. (2012). *The pesticide manual : a world compendium*.

Muñoz-Quezada, M. T., Lucero, B. A., Barr, D. B., Steenland, K., Levy, K., Ryan, P. B., Iglesias, V., Alvarado, S., Concha, C., Rojas, E., & Vega, C. (2013). Neurodevelopmental effects in children associated with exposure to organophosphate pesticides: A systematic review. *NeuroToxicology*, *39*, 158-168.

Navaei-Nigjeh, M., Asadi, H., Baeeri, M., Pedram, S., Rezvanfar, M. A., Mohammadirad, A., & Abdollahi, M. (2015). In vitro protection of human lymphocytes from toxic effects of chlorpyrifos by selenium-enriched medicines. *Iran J Basic Med Sci*, *18*(3), 284-291.

Parliament of the Republic of Serbia (2005). Law on Health Care. *Official Gazette of the Republic of Serbia*, vol. 107 (pp. 112-161): Official Gazette of the Republic of Serbia.

Roy, T. S., Andrews, J. E., Seidler, F. J., & Slotkin, T. A. (1998). Chlorpyrifos elicits mitotic abnormalities and apoptosis in neuroepithelium of cultured rat embryos. *Teratology*, *58*(2), 62-68.

Sai, L., Li, X., Liu, Y., Guo, Q., Xie, L., Yu, G., Bo, C., Zhang, Z., & Li, L. (2014). Effects of chlorpyrifos on reproductive toxicology of male rats. *Environmental Toxicology*, *29*(9), 1083-1088.

Soltaninejad, K., & Abdollahi, M. (2009). Current opinion on the science of organophosphate pesticides and toxic stress: a systematic review. *Med Sci Monit*, *15*(3), RA75-90.

Surralles, J., Xamena, N., Creus, A., Catalan, J., Norppa, H., & Marcos, R. (1995). Induction of micronuclei by five pyrethroid insecticides in whole-blood and isolated human lymphocyte cultures. *Mutation Research*, *341*(3), 169-184.

Suvarchala, G., & Philip, G. H. (2016). Toxicity of 3,5,6-trichloro-2-pyridinol tested at multiple stages of zebrafish (Danio rerio) development. *Environmental Science and Pollution Research*, *23*(15), 15515-15523.

Turtoi, M. (2013). Ultraviolet light treatment of fresh fruits and vegetables surface: A review. *Journal of Agroalimentary Processes and Technologies*, *19*(3), 325-337.
WHO (2015). WHO SPECIFICATIONS AND EVALUATIONS FOR PUBLIC HEALTH PESTICIDES: CHLORPYRIFOS. (pp. 1-53).
Wood, S. J., & Osborne, R. H. (1991). Is sulfotep a proctolin receptor antagonist? *Pesticide Science*, *32*(4), 485-491.
Zabar, R., Sarakha, M., Lebedev, A. T., Polyakova, O. V., & Trebse, P. (2016). Photochemical fate and photocatalysis of 3,5,6-trichloro-2-pyridinol, degradation product of chlorpyrifos. *Chemosphere*, *144*, 615-620.

Figure captions

Fig. 1. The chromatograms recorded after 0 (a), 14 (b), 36 (c), 80 (d) and 180 min (e) of UV-C light irradiation of 7.74×10^{-5} M CPF in TCPF in MeOH:H_2O=1:1. Inset: The chromatogram of analytical standards of CPF (7.1×10^{-6} M) and CPO (6.1×10^{-7} M).

Fig. 2. a) Inhibition curves of AChE induced by TCPF (1 - square), EW (2 - circle) and EC (3 - triangle) formulations, CPF (4) and CPO (5); Change of AChE activity (bold line), % of CPF comparing to initial CPF concentration (solid symbols) and CPO concentration (open symbols with plus) as the function of irradiation time for irradiated samples containing initially b) 3.87×10^{-6} CPF in TCPF; c) 4.32×10^{-6} CPF in EW and d) 3.47×10^{-6} M CPF in EC (final concentrations in enzyme assay)

Fig. 3. a) Concentration dependent increase of MDA level in human lymphocytes treated with unirradiated TCPF (square), EW (circle) and EC (triangle) formulations; MDA level alterations (bold line) in lymphocytes treated with irradiated b) TCPF, c) EW and d) EC formulations as a function of irradiation time. The MDA values are expressed as percentage of control (non-irradiated initial parent compounds) set to 100% (t_{irr} = 0 min); CPF (solid symbols) and CPO (open symbols with plus) represent the percentage of initial CPF concentration in irradiated samples.

Fig. 4. a) Activity of catalase in blood cultures treated with unirradiated TCPF (square), EW (circle) and EC (triangle) formulations; Alteration of catalase activity in lymphocytes (bold line) treated with irradiated b) TCPF, c) EW and d) EC formulations as a function of irradiation time. The values are expressed as percentage of control (non-irradiated initial parent compounds) set to 100% (0 min); CPF (solid symbols) and CPO (open symbols with plus) represent the percentage of initial CPF concentration in irradiated samples.

Fig. 5. a) Incidence of micronuclei (MN/1000 BN cells) in human lymphocytes treated with unirradiated TCPF (square), EW (circle) and EC (triangle) formulations; Alteration of the incidence of micronuclei in lymphocytes (bold line) treated with irradiated b) TCPF, c) EW and d) EC formulations as a function of irradiation time. The values are expressed as percentage of control (non-irradiated initial parent compounds) set to 100% (0 min); CPF (solid symbols) and CPO (open symbols with plus) represent the percentage of initial CPF concentration in irradiated samples.

Fig.6. a) A cytokinesis-block proliferation index (CBPI) in human lymphocytes treated with unirradiated TCPF (square), EW (circle) and EC (triangle) formulations; Alteration of CBPI in human lymphocytes (bold line) treated with irradiated b) TCPF, c) EW and d) EC formulations as a function of irradiation time. The values are expressed as percentage of control (non-irradiated initial parent compounds) set to 100% (0 min); CPF (solid symbols) and CPO (open symbols with plus) represent the percentage of initial CPF concentration in irradiated samples.

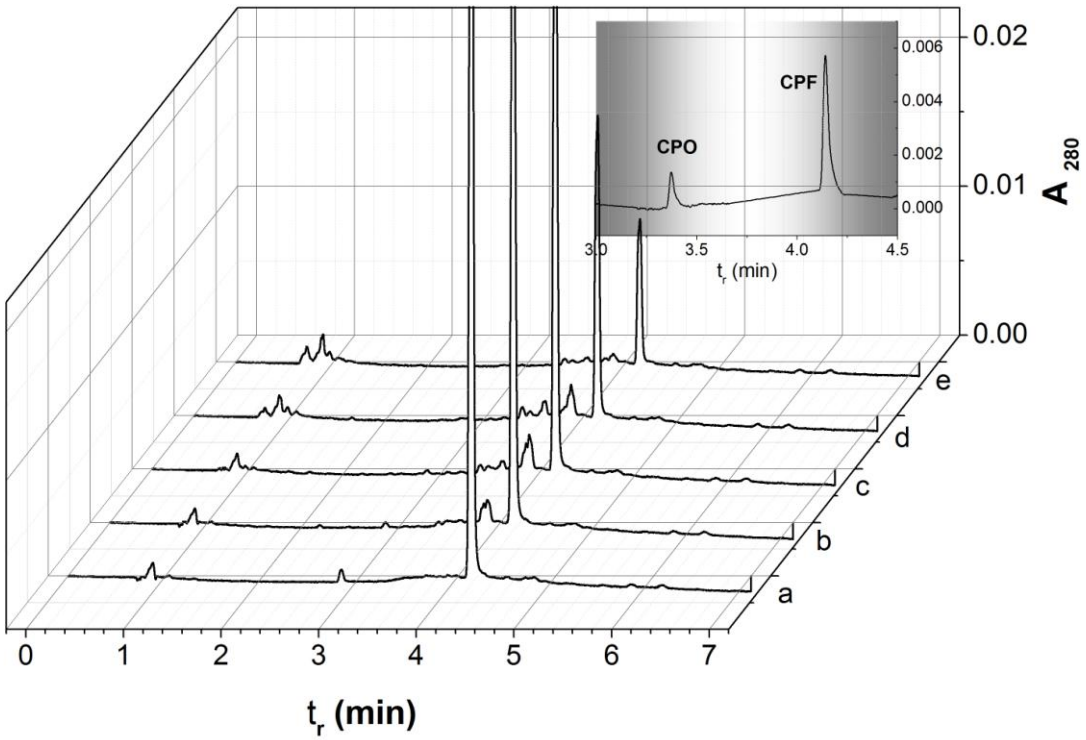
CPO
CPF
0.006
0.004
0.002
0.000
3.0
3.5
4.0
4.5
t_r (min)
0.02
0.01
0.00
A_{280}
e
d
c
b
a
0
1
2
3
4
5
6
7
t_r (min)

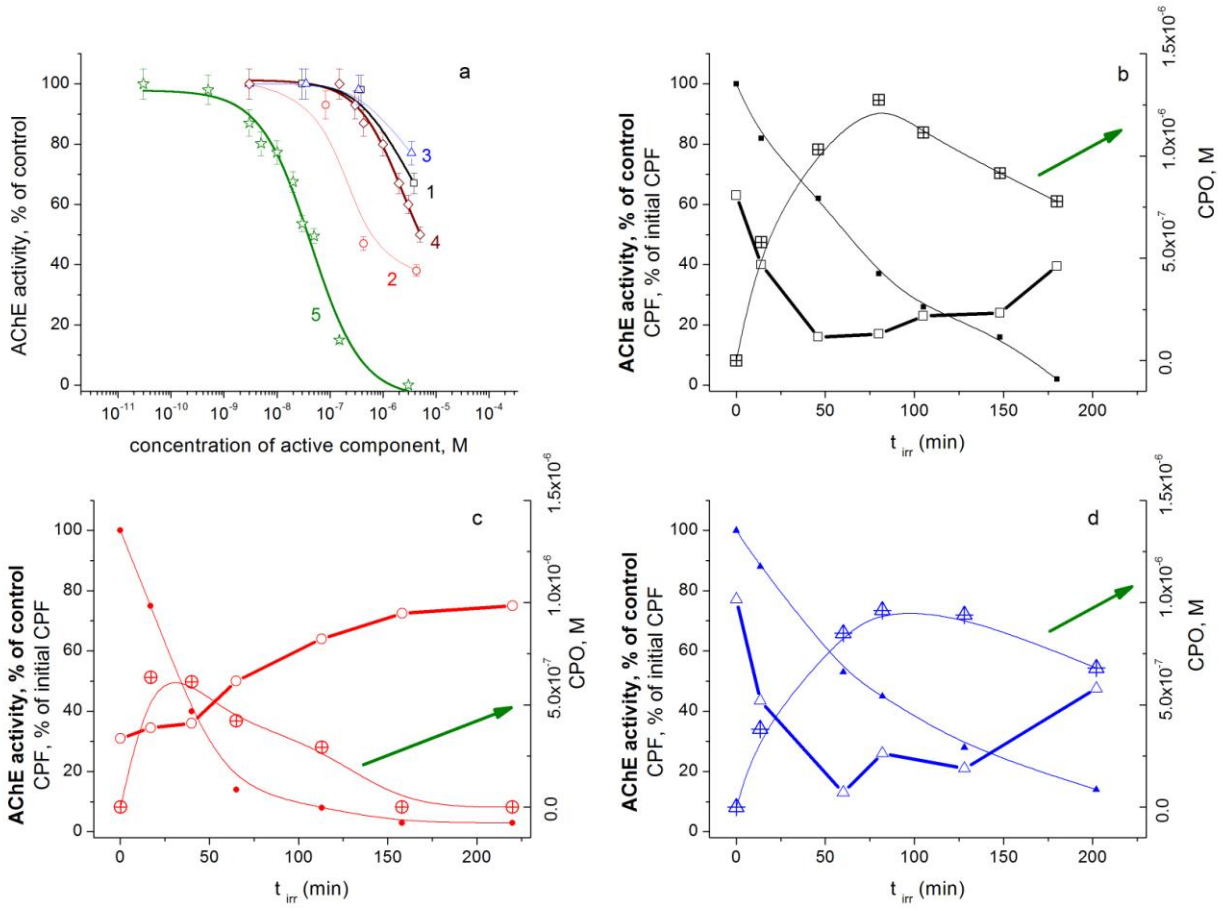

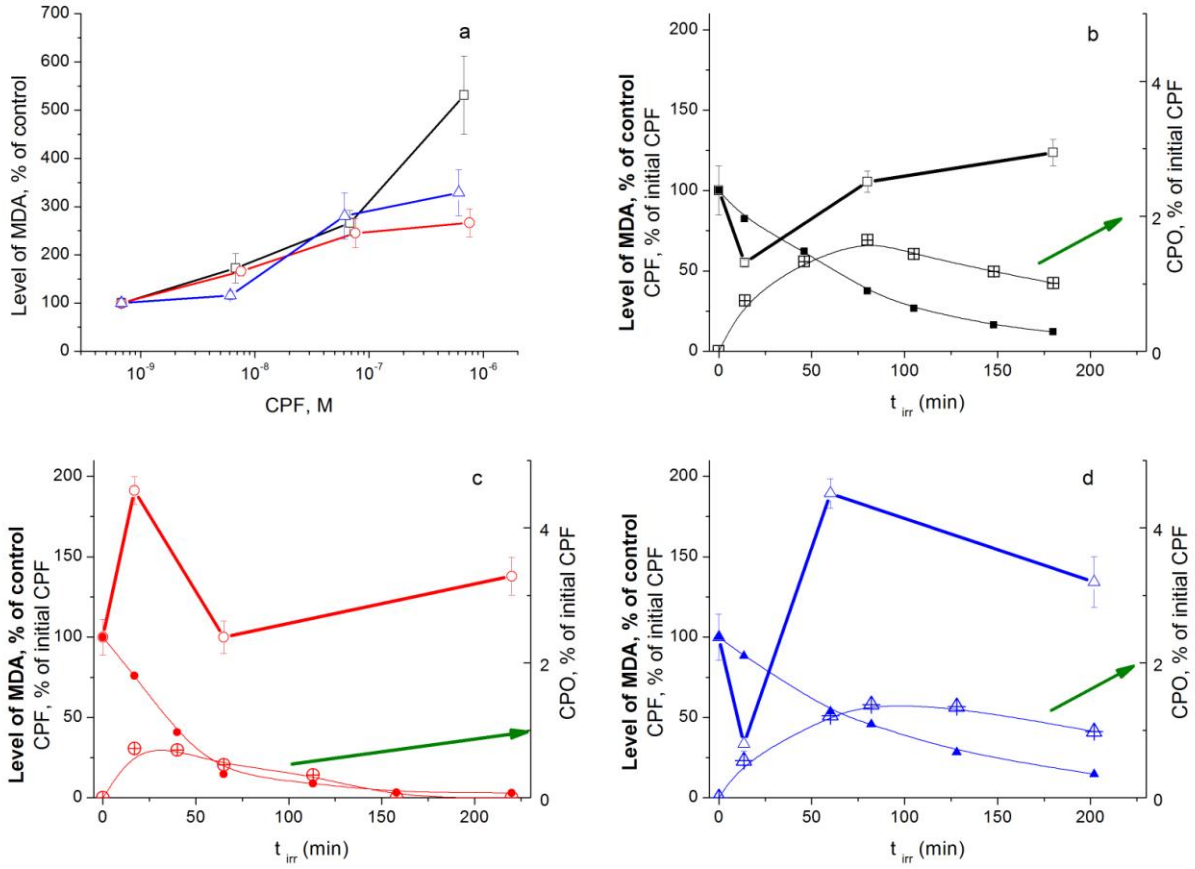

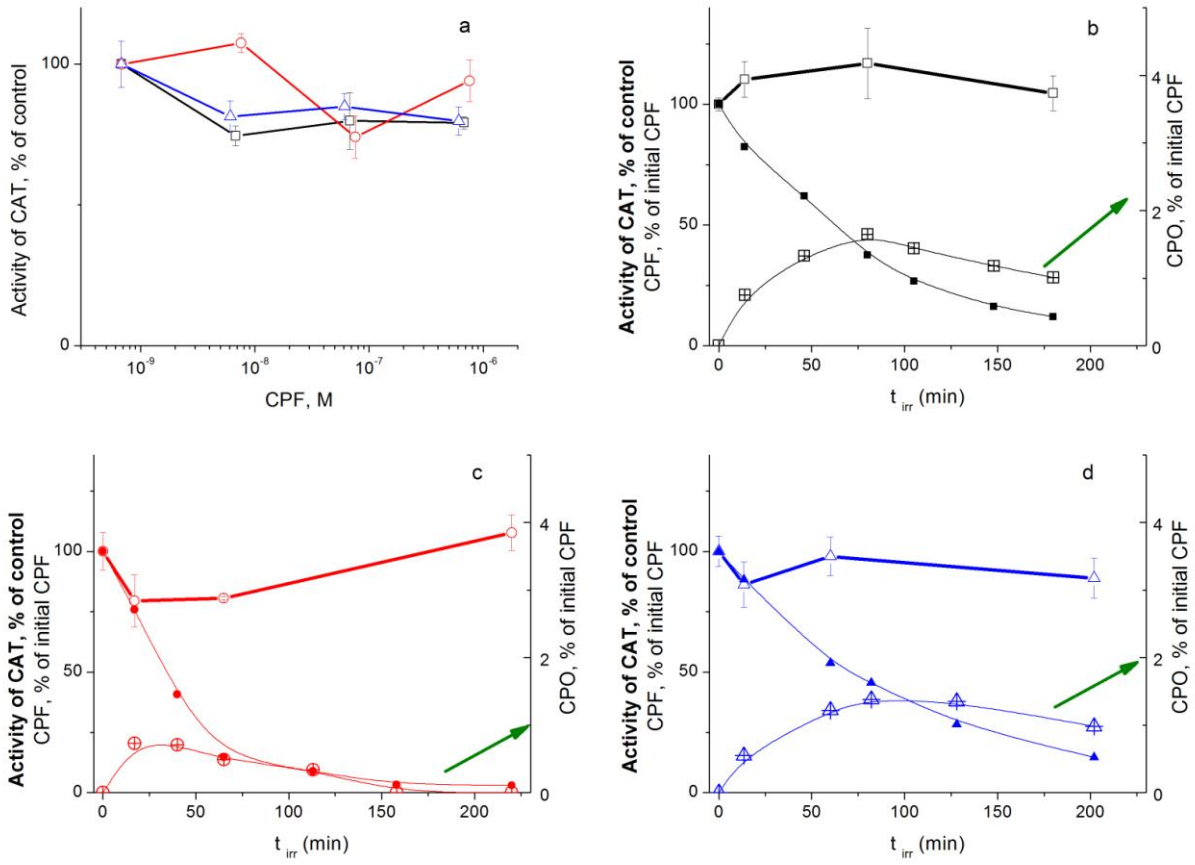

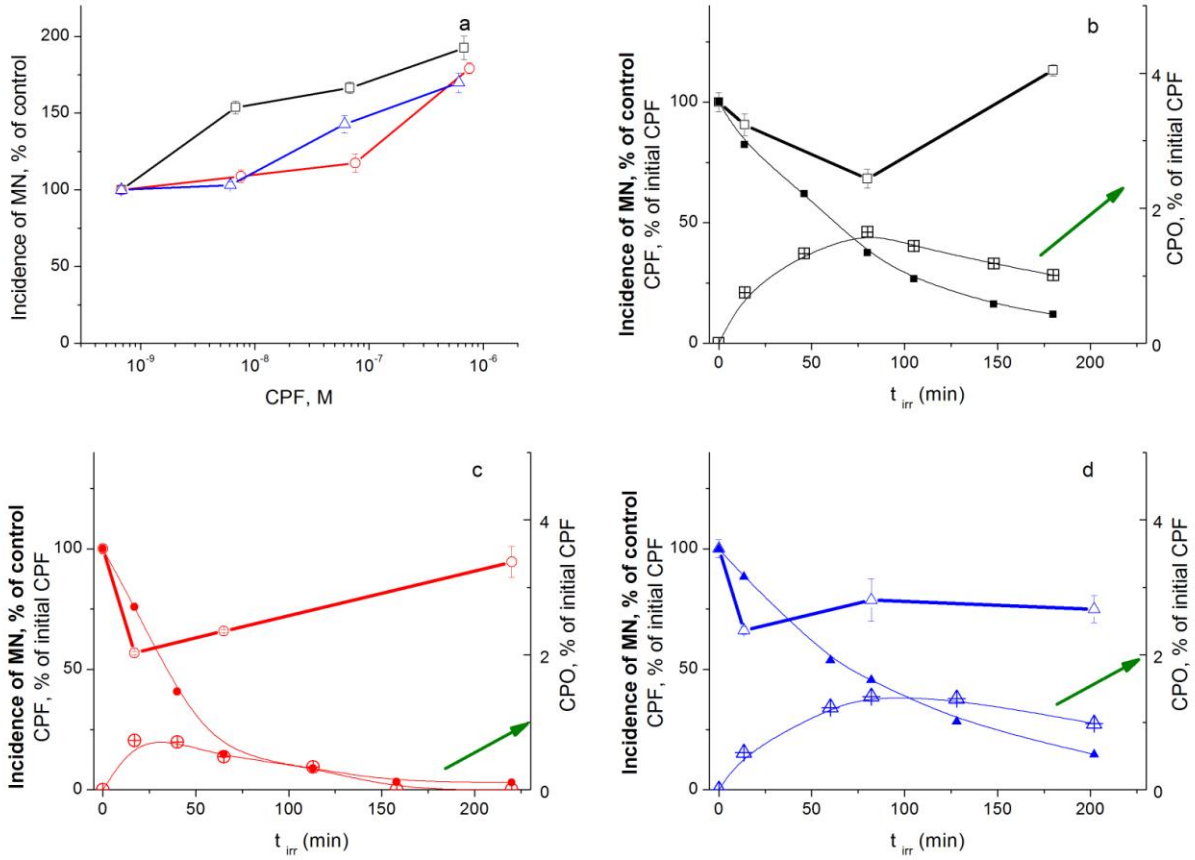

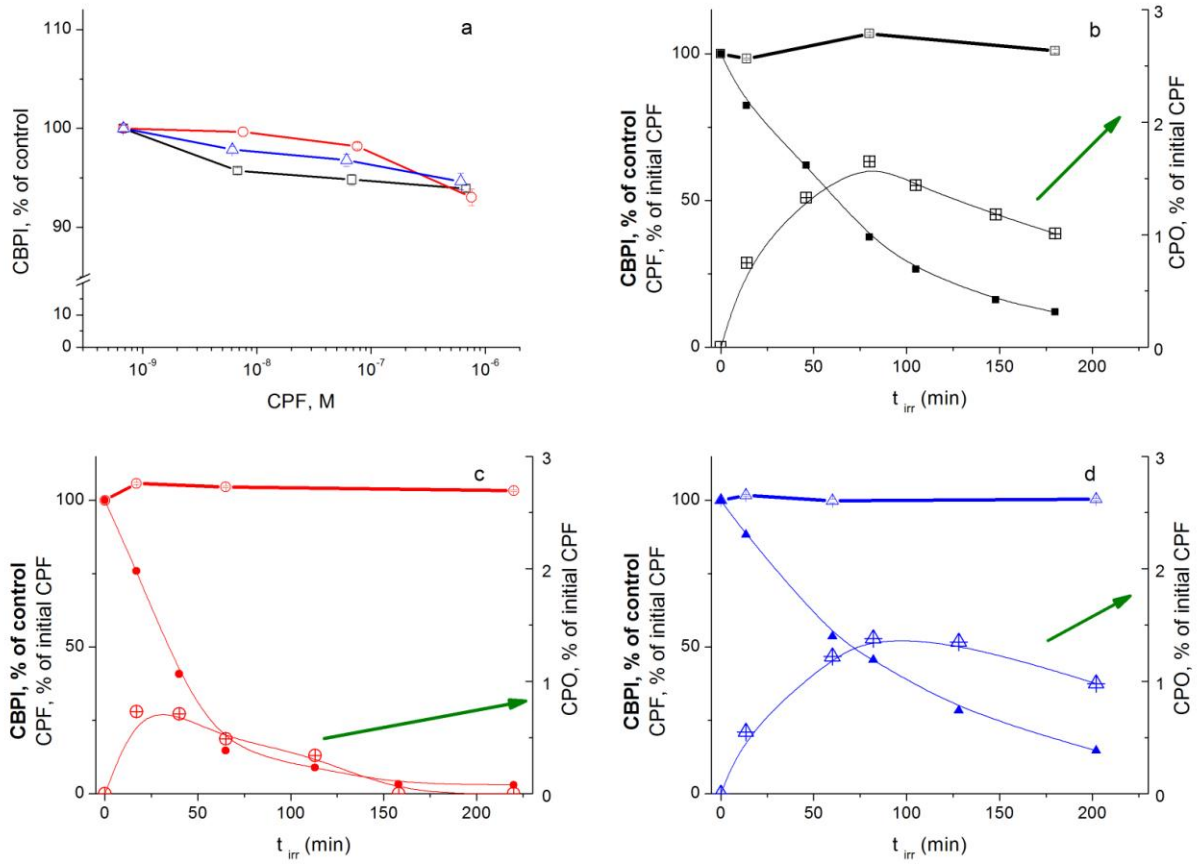

Highlights

- UV-C irradiation of chlorpyrifos and its formulations enhances their toxic effects
- Irradiated chlorpyrifos and its formulations induce DNA damage and oxidative stress
- Technical chlorpyrifos is a more potent genotoxic inducer than its formulations
- Irradiated chlorpyrifos formulations affect acetylcholinesterase differently